

RESEARCH ARTICLE

Optimal C-type filter design for wireless power transfer system by using support vector machines

Haris Calgan *

Department of Electrical-Electronics Engineering, Balikesir University, Turkey
haris.calgan@balikesir.edu.tr

ARTICLE INFO

Article history:
Received: 18 January 2023
Accepted: 31 March 2023
Available Online: 9 July 2023

Keywords:
C-type power filter
Support vector machine
Optimization
Wireless power transfer
Electrical vehicle

AMS Classification 2010:
68Q32, 68T01, 62J02

ABSTRACT

The rapid increase in the number of Electrical Vehicles (EVs) will bring difficulties in the management of charging process and pose serious grid problems at low voltage levels. Particularly, with employment of wireless power transfer (WPT) system in a charging station, harmonic interference will increase. The main reason of that poor power quality lies on high frequency square wave output of transmitter side of WPT. In this study, a support vector machine (SVM) is proposed to design an optimal C-type passive filter in order to mitigate voltage and current total harmonic distortions (THD) of WPT system. Hereby, SVM-based model is constructed which consists of THD indices and power factor (PF) as outputs whereas filter parameters are inputs. The main aim of optimization process is minimization of distortions and correction of PF while searching the filter parameters. Particle swarm optimization (PSO) algorithm is employed to find the optimal filter parameters. To show the efficiency of proposed method, simulation studies are carried out on Matlab[®]/Simulink[™] environment. It is observed that voltage total harmonic distortion (THD_v) and current total harmonic distortion (THD_i) are calculated as 1.03%, 2.23%, respectively, and the power factor is improved to 0.995% when the designed C-type filter is utilized.



1. Introduction

In recent years, carbon-based energy generation systems that cause environmental damage such as global warming, air pollution, water pollution, etc. have begun to replace systems that produce electrical energy through renewable and environmental friendly [1]. In addition, vehicles using carbon-based fuels are one of the important causes of environmental pollution. In order to solve this problem, it is great importance that vehicles working with electric energy should become widespread. In the event that the use of electric vehicle (EV) becomes widespread, another problem, which is efficient charging station design and easy access to stations, comes to the fore. According to the IEC61851 standard prepared for electric vehicle charging stations (EVCS), it is allowed to draw currents up to 32 A in residential uses and draw up to 250 A in alternating current in different charging modes. However, the rapid increase in the number of EVs will bring difficulties in the management of the charging process and pose serious grid problems at low voltage levels [2, 3].

Increasing load demand will create the need for additional facility investment. By using various heuristic algorithms, the effects of EVs on the distribution grid can be reduced and the load profile can be slightly smoothed [4]. However, it is still difficult to meet the desired electrical energy need without a facility investment.

Wireless charging methods, on the other hand, have come as a major innovation to the EV industry. Compared to conventional charging units, they do not require power connection. Wireless power transfer (WPT) is divided into static and dynamic structures. Static wireless power transfer systems by placing a single coil under a parked vehicle were proposed by General Motors in 1998 [5]. WPT is a safer and more convenient method for electrical charging due to its cable-free structure and resistant to environmental factors such as water and dust. When the reported studies are examined, it is seen that WPT is frequently employed in charging EVs. Li and Mi [6] present a study on magnetic coupling design in wireless power

*Corresponding author

transfer for EVs. They show the circuit compensation with power control via converters. Musavi and Eberle [7] compared the current wireless charging technologies for EVs on the basis of values such as efficiency, cost, capacity, and system complexity. They present two different wireless/built-in fast charging circuit models which are integrated into the vehicle, separately for passenger cars and large public transportation vehicles. Sun et al. [8] review existing wireless charging technologies for EVs and their applications. They examine different types of wireless charging applications for EVs and their economic feasibility is analyzed. In addition, electromagnetic field shielding methods for WPTs are also investigated.

Most of the aforementioned WPT applications include DC-DC or AC-DC converters. In fact, AC-DC converters in WPT systems are more convenient for grid-connected applications [9]. However, these converters contain high-frequency triggering and induce harmonic distortion on the voltage and current waveforms. These harmonics may cause unexpected impacts on the equipment in the system such as heating, malfunction on the actuator and line loss of the network [10]. Therefore, filters are generally designed in order to cope with these harmonics. Among the power filter types, passive filters are easy to implement and cost-effective. So, they are widely employed in power systems. Further, they are preferred to handle the harmonics particularly in electrical vehicle charging station. In this regards, Yang et al. [11] design a single-tuned passive filter which combines reactance and capacitor and creates a low resistance channel for specific order harmonics. According to their analyses, they find that the fifth and seventh orders are the most part of harmonics of EVCS. By using the designed single-tuned filter they decrease the THD_i to a low level. Zao and Yue [12] take the effects of the electric vehicle six-pulse rectifier charger into account and design single-tuned filter as well as high pass filter. Their simulation results show that a good harmonic suppression is achieved with the presented passive filter. Khudher et al. [13] present the design of output filter with shunt passive filters to decrease impact of electrical car charging stations on power grid harmonics. They reduce the THD_i from 46.19% to 3.73% by combining the double-tuned filters with high pass filter.

Alongside the conventional filters such as combination of single-tuned LC and high pass filter, parallel resonance can be avoided in the system by using C-type passive filter. Furthermore, it has lower loss than high-pass filter at fundamental frequency [14]. Due to these advantages, it is widely used in different applications such as loading capability improvement of transformers under non-sinusoidal conditions [15], filtration of higher harmonics injected into the transfer system by arc furnaces [16] and capacity reduction of hybrid power quality conditioner in co-phase traction power system [17].

According to the author's knowledge, there is lack of study in the implementation of C-type passive filter for WPT system which is the main contribution of this study. However, an optimal design of a C-type filter requires the analysis of system with single-phase equivalent circuit. Therefore, most of the equivalent circuit parameters such as linear impedance parameters of load and Thevenin equivalents have to be known. However, some studies construct a model between THD values and specified input parameters. In this context, Response Surface Method [18] and comparison of artificial neural network and SVM [19] are reported. However, in [19], SVM method is employed only for harmonic estimation.

In this study, SVM-based optimal design of C-type passive filter is proposed for an EVCS which contains AC-DC converter, a high frequency single phase inverter and WPT. The main advantage of the proposed method is no need of equivalent circuit parameters of the system while determining the model. THD_v , THD_i and PF are chosen as output parameters of the model whereas the filter parameters are assigned as input parameters. Afterwards, a traditional PSO method is applied on that model to minimize THD_v and THD_i as well as to maximize PF.

The organization of this manuscript is as follows: Section 2 describes EVCS with WPT. Section 3 defines the main problem of this study with THD indices. Section 4 explains C-type passive filter design. Section 5 details SVM-based modeling and PSO based optimization studies. Section 6 contains results and discussion. Section 7 is the conclusion.

2. Description EVCS with WPT system

The proposed EVCS basically contains three-phase rectifier, DC-link buffer, full-bridge resonant inverter, series-resonant LC tank, vehicle-side rectifier. Figure 1 shows the general scheme of system with C-type filter which is detailed in the next sections. In this system, proposed resonant inverter is grouped as Class D and is most popular for practical WPT systems [20].

As shown in Figure 1, proposed EVCS has series-series compensation topology. In this method, L_p , C_p , L_s and C_s stand for primary, secondary coils and compensated capacitors, respectively. If the primary and secondary coil currents are defined as I_p and I_s , effect of the secondary impedance to the primary side is expressed as in Eq. (1)

$$Z_r = \frac{-j\omega MI_s}{I_p} = \frac{\omega^2 M^2}{Z_s} \quad (1)$$

where M denotes the mutual inductance and calculated by

$$M = k\sqrt{L_p L_s} \quad (2)$$

where k is the coupling coefficient and ranged between 0 and 1 ($0 < k \leq 1$). The impedance of the secondary side Z_s is determined as in Eq. (3).

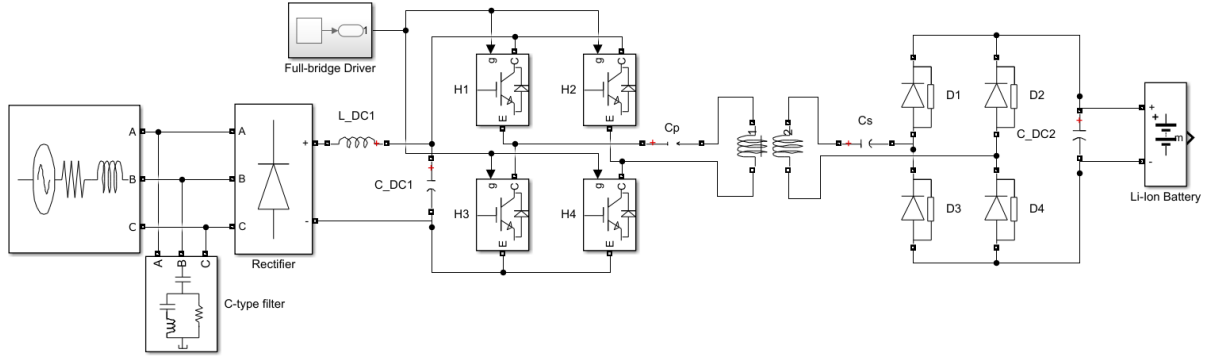


Figure 1. Block scheme of the EVCS

$$Z_s = j\omega L_s + \frac{1}{j\omega C_s} + R_L \quad (3)$$

where R_L is the load resistance and resonant frequency is calculated by $\omega_r = 1/\sqrt{L_s C_s}$. Consequently, the equivalent load impedance on the primary side is determined as in Eq. (4).

$$Z_s = j\omega L_p + \frac{1}{j\omega C_p} + Z_r \quad (4)$$

Alongside the WPT of EVCS, 3-phase, 380 V, 50 Hz AC grid voltage is rectified to 360 V_{dc} on the DC bus. Afterwards, it is inverted to 360 V, 30 kHz square wave AC voltage by means of full bridge resonant inverter. This signal is transferred to secondary side wirelessly. Lastly, vehicle-side converter rectifies the AC voltage to 360 V DC voltage in order to charge the lithium-ion batteries. Equivalent circuit parameters of the designed WPT system are given in Table 1. With given circuit parameters, resonant frequency is calculated as 30 kHz, approximately.

Table 1. The equivalent circuit parameters of WPT

Parameter	Value
C_p	105.74e ⁻⁹ F
C_s	109.69e ⁻⁹ F
L_p	266.16e ⁻⁶ H
L_s	256.79e ⁻⁶ H
M	85.46e ⁻⁶ H

3. Problem definition

Regarding the presented EVCS, full-bridge resonant inverter converts the 360 V DC input into 360 V AC square wave output. The Fourier transform of the converted square wave is given by Eq. (5) [21].

$$U_{TX} = \frac{4}{\pi} U_{DC} \sum_{n=1,3,5}^{\infty} \frac{1}{n} \sin(n\omega_r t) \quad (5)$$

where U_{TX} is the output voltage of full-bridge resonant inverter as well as the input voltage of the WPT transmitter side. U_{DC} is the input of inverter when ω_r is chosen as resonant frequency and n is the harmonic order. It can be seen from Eq. (5) that U_{TX} includes harmonics. According to the harmonic analysis of WPT system given in [21], despite the harmonic current is reduced effectively by adjusting Q value of the resonant

circuit, in some cases, harmonic current required to be reduced. So, the balance between Q value and harmonic voltage loaded on the transmitter coil should be adjusted accurately. Moreover, fundamental energy to harmonic energy ratio is given by Eq. (6).

$$\frac{P_{Harmonic}}{P_{Fundamental}} = \frac{1}{n^2} \frac{1}{\left(n\omega_r \frac{L}{R}\right)^2 \left(k - \frac{1}{k}\right)^2 + \frac{1}{k^2}} \quad (6)$$

It can be deduced from Eq. (6) that the energy of harmonic transmission decreases since the k decreases. However, when the k is chosen around 0.9, maximum harmonic transmission ratio is observed [21]. It is also proven that when the harmonic-related reactive power accumulation increases, efficiency of the inverter-driven WPT system decreases. So, an appropriate control for inverter can overcome the harmonic related reactive power accumulation [22]. Additionally, aforementioned studies generally employ DC source and focus on harmonics on the WPT side. Since the EVCS is fed by the grid, the energy consumed via WPT draws non-sinusoidal currents from the grid. THD_i and THD_v can be calculated as in Eqs. (7) and (8) considering the fundamental frequency active power (P_1), reactive power (Q_1), fundamental frequency RMS current (I_1) and sinusoidal-rated supply voltage (V_1) [23].

$$THD_i = \frac{\sum_{n \neq 1} I_n^2}{I_1} \quad (7)$$

$$THD_v = \frac{\sum_{n \neq 1} V_n^2}{V_1} \quad (8)$$

where I_n and V_n stand for n^{th} harmonic current and voltage. Additionally, PF can be calculated as in Eq. (9) in terms of both powers.

$$PF = \frac{P_1}{V_1 I_1} = \cos \phi_1 \quad (9)$$

where ϕ_1 denotes phase angle difference between fundamental frequency voltage and current. To avoid drawing of harmonically contaminated currents and improve PF, C-type passive filter is designed to fulfill the desired criteria which are minimization of THD_v, THD_i as well as maximizing the PF.

4. C-type passive filter design

Circuit of the typical C-type passive filter is given in Figure 2. Design procedure of the filter begins with the determination of reactive power Q_l at fundamental frequency f_0 , which is 50 Hz, regarding to nominal voltage U_n and tuning frequency f_n .

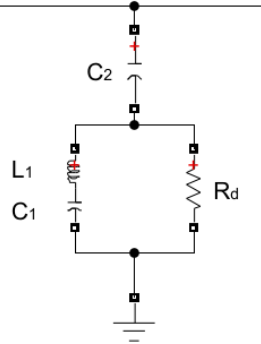


Figure 2. Circuit of the C-type filter

After specifying the necessary parameters, C_2 should be chosen large enough in order to meet the desired reactive power of the system. Afterwards, C_1 is calculated by means of following equation [24].

$$C_1 = C_2 \left[\left(\frac{f_n}{f_0} \right)^2 - 1 \right] \quad (10)$$

Then, series L_1 - C_1 are tuned to f_0 as follows:

$$f_0 = \frac{1}{2\pi\sqrt{L_1 C_1}} \quad (11)$$

From Eq. (11), L_1 value is calculated since the tuning is realized. In order to have more effective filter a low value quality factor Q at the designed frequency f_n is chosen within 2 or 3. Damping resistance R_d is specified as in Eq. (12).

$$R_d = \frac{2\pi f_n L_1}{Q} \quad (12)$$

It is seen from Eqs. (10), (11) and (12) that the design problem of a C-type passive filter can be solved via foreknowledge of the system characteristics. In this study, without knowledge of these parameters an optimal filter design is aimed which employs a support vector machine-based modeling technique. Note that, alongside the C-type passive filter a serial connected input inductance L_i is also employed in the system.

5. Support vector machine-based optimization of C-type passive filter

This study intends to find optimal C-type passive filter parameters. While searching filter parameters, THD_v , THD_i values are aimed to be minimized and PF values is aimed to be close to 1. Hence, SVM regression method is utilized to model the system, PSO is operated to reach optimal filter parameters. The entire modeling and optimization processes are given as flowchart in Figure 3. The proposed method mainly targets to obtain

optimal C-type filter parameters. But, modeling with high accuracy is the key procedure. Since the SVM is not able to well perform in estimation, PSO algorithm will not give the best filter parameters. Therefore, high accuracy in modeling is necessary to be successful in optimization. After ensuring the model certainty, for a given search space, PSO is employed to reach desired metrics by means of calculating the best filter parameters. The details of modeling and optimization are reported in subsections.

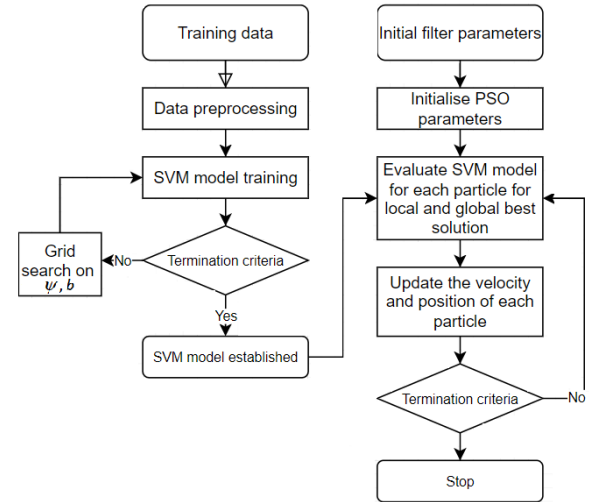


Figure 3. Flowchart of SVM-based optimization of C-type filter parameters

5.1. Support vector machine-based modelling

There are lots of machine learning-based modeling method in literature such as RSM [25], Artificial Neural Network [26] and Long Short-term Memory [27]. Support vector machine is also one of a machine learning methods and was proposed presented in 1995 by Cortes and Vapnik [28]. The general structure of an SVM is given in Figure 4. It is widely employed in the literature for the purpose of estimation, analysis and regression problems [19]. The main advantage of SVM is showing better performance against getting stuck with local minimum problem [29].

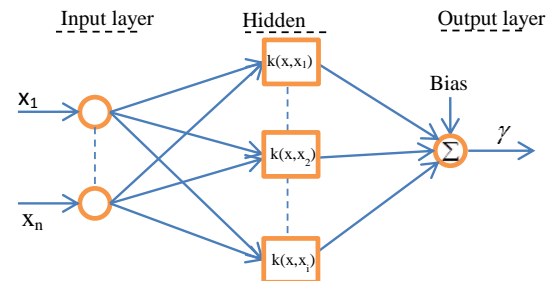


Figure 4. General scheme of SVM

Support vector regression (SVR) is an utilization of SVM and uses distinct kernel functions such as polynomial, radial basis function, sigmoid and linear. Since a training dataset contains input vector x_i and

output vector γ_o , regression model can be formed as given in Eq. (13).

$$\gamma_o - \psi^T \theta(x_i) + b \quad (13)$$

where ψ , b , $\theta(\cdot)$ stand for weighting vector, bias and nonlinear mapping function, respectively. In order to determine weighting parameters of regression model, the distance between margin and input vector that lie on the wrong side must be measured. Furthermore, the confidence interval and the empirical risk should be adjusted by penalty parameters. These two requirements yield a minimization problem as given in Eq. (14) to be solved [30].

$$\frac{1}{2} \psi^2 + k_p \sum_{i=1}^N \xi_i + \xi_1^{(*)} \quad (14)$$

where ξ_i denotes the slack variable and k_p is a constant penalization parameter. Weighting parameters are calculated when the function given in Eq. (14) is minimized. Lastly, Lagrange multipliers are introduced to solve the support vector regression problem.

Since this study aims to determine optimal C-type passive filter, input-output data of SVM are appointed as filter parameters and harmonic values, respectively. To elaborate more, filter parameters which are given in Eqs. (10), (11) and (12) are denoted as inputs, THD_v, THD_i and PF values are specified as outputs. Training dataset is formed by input-output data which is derived from simulation studies. Matlab[®]/Simulink[™] program is chosen as simulation platform and min-max values of inputs are determined as given in Table 2. Considering the increment (step) values, simulation is run 180 times and THD_v, THD_i and PF values are recorded to be used in modeling procedure.

Table 2. Filter parameters constraints

Parameter	min	step	max
C_2	$1.2e^{-4}$	$2e^{-5}$	$2e^{-4}$
f_n/f_0	3	2	7
Q	3	2	7
L_i	$5e^{-3}$	$5e^{-3}$	$2e^{-2}$

After constructing the input-output training data set Matlab[®] 'fitrsvm' command is employed to train SVM regression model. Note that normalization pre-process on the dataset is applied before training by using maximum values of each parameter as given in Table 2. Data mapping is occurred with Gaussian kernel functions and all elements of the predictor matrix divided by the value of appropriate KernelScale (auto). Using the chosen specifications, SVM model is obtained with 0.94 r-squared (R^2). To summarize, SVM predicts harmonic distortions and power factor with the high accuracy for the given filter parameters. It proves that the model can be used in optimization precisely.

5.2. Particle swarm optimization

PSO method is used for different applications in industry such as renewable energy [31], automation [32] and adaptive wireless power transfer [33]. Specifying the C-type filter parameters is a complex problem due to the nonlinearity of the EVCS. The performance of the filter can be improved by reducing THD_i and THD_v likewise by approximating to 1 in terms of PF. Additionally, it is well-known fact that THD_i and THD_v should be kept under limitation defined by IEEE Standard 519-2014 [34]. The THD_i limit is recommended as 8% when the ratio between maximum short-circuit current (ISC) and maximum demand load current (IL) at common coupling point (PCC) is less than 20. On the other hand, THD_v limit is defined as 5% since the bus voltage is less than 1 kV. Considering these limitations and handling PF as a percentage, the fitness function (FF) is designed by taking the limits equal to each other as 5%. Therefore, in this study, after well modeling of the EVCS with SVM, a fitness function is identified to be minimized and as given in Eq. (15). Note that, THD_i, THD_v and PF values given in Eq. (15) are predicted by SVM during the optimization process.

$$FF = w_1 THD_i + w_2 THD_v + w_3 (1 - PF) \quad (15)$$

where w_1 , w_2 , w_3 are weightings of each parameter. As shown in Eq. (15), optimization problem has two parameters to be minimized and third parameter to be maximized which yields multi-objective optimization problem. However, considering the significance and goal value of each parameter, the problem can be converted to a single objective optimization by choosing the weightings equal. Hereby, minimization of THD values and maximization of PF can be done with equal importance. A set of lower and upper bounds on the design variables are given in Table 2. The optimization problem to get mentioned values under predefined constraints can be summarized as given in Eq. (16).

In this problem, search space is defined by Ω . The problem has four filter parameters to be optimized, where their general form can be indicated as $f_{p_{\min}} \leq fp \leq f_{p_{\max}}$. Note that C_1 and R_d are not included in optimization problem. Because, these two parameters are calculated by Eqs. (10) and (12), since the given parameters are determined.

$$\begin{aligned} & \underset{fp \in \Omega}{\text{Min}} FF(fp) \\ & \text{subject to : } \Omega \left\{ \begin{array}{l} 1.2e^{-4} \leq C_2 \leq 2e^{-4} \\ 3 \leq f_n / f_0 \leq 7 \\ 1e^{-3} \leq Q \leq 7 \\ 5e^{-3} \leq L_i \leq 2e^{-2} \end{array} \right. \quad (16) \end{aligned}$$

Classical PSO algorithm of Matlab[®] is used in this study. The parameters of PSO are given in Table 3. As mentioned before, applied SVM is done with normalized dataset during the modelling step. Therefore, each parameter of fp is normalized using the same method. After several optimization processes, best FF is obtained as 3.27 when the filter parameters are calculated as given in Table 4. By using 'rng' function of Matlab[®], random number generation is controlled for reproducibility. Hereby, it is confirmed in each trial that, PSO is started with different initialization which yields not trapping by a local minimum solution.

Table 3. PSO tuning parameters

Parameter	Value
Function tolerance	$1e^{-6}$
Initial swarm span	2000
Min neighbors fraction	0.25
Self-adjustment weight	1.49
Swarm size	[100,300]

Table 4. Obtained filter parameters

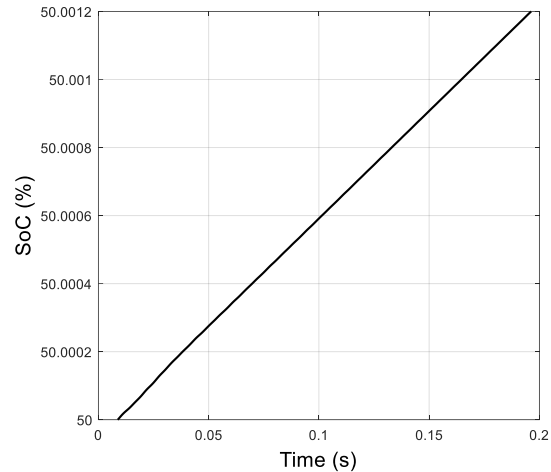
Parameter	Value
C_2	$1.6e^{-4}$ F
C_1	$9.6e^{-3}$ F
L_1	$1.1e^{-3}$ H
L_i	$2e^{-2}$ H
R_d	121 Ω

Regarding to the obtained C-type filter, performance of the system is analyzed in the next section.

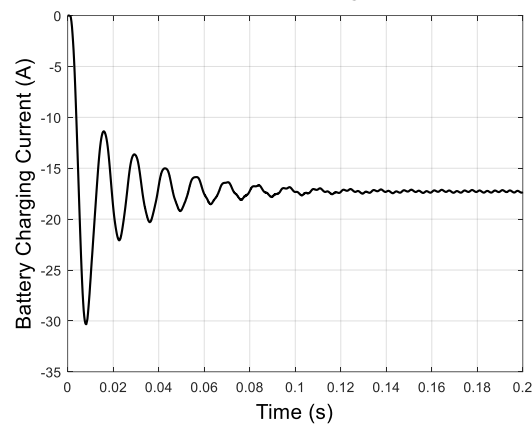
6. Results and discussion

This section presents and compares numerical results obtained by simulating EVCS with and without C-type passive filter. Matlab[®]/Simulink[™] environment is employed for simulation studies. For the simulated EVCS, the equivalent circuit parameters are chosen as described in Section 2. Additionally, lithium-ion battery with a rectifier is connected to the secondary side of WPT. The system is supplied by three phase grid voltage which is 400 V in fundamental frequency and specifications of battery are as follows; nominal voltage=360 V, rated capacity=100 Ah, initial state-of-charge (SoC)=50%, battery response time=10 s, battery internal resistance=0.036 Ω .

Initially, the system is simulated without passive filter. Figure 5 shows the charging current and state of charge of lithium-ion battery. It is seen from figure that battery drawn around 15 A from DC link and keep being charged. It is clear that charging process works effectively.



(a) State of charge



(b) Change in charging current

Figure 5. Charging of the battery without C-type filter

In the case of operating the EVCS without filter, waveform of the voltage at the point of common coupling is demonstrated in Figure 6a with harmonic spectrum. The magnitude and harmonic spectrum of current drawn from the grid is obtained as illustrated in Figure 6b. It is seen from Figure 6 that THD_v and THD_i are measured as 13.99% and 22.23%, respectively. The system has also low PF which is measured as 0.91. It is clear that THD values are above the limits and should be mitigated. Moreover, mitigation of harmonics may increase the effectiveness of the WPT and may accelerate the battery charging process.

Measured voltage and current with harmonic spectrums are illustrated in Figure 7 when the system is operated with designed C-type filter. In this case, voltage and current harmonics are reduced to 1.03% and 2.23%, respectively. PF is improved to 0.995. The absolute differences between the results show that the designed C-type filter keeps the THD_v , THD_i indices and PF within limits defined by IEEE Standard 519-2014. So, the results show that optimal C-type filter is determined effectively by using the SVM-based approach.

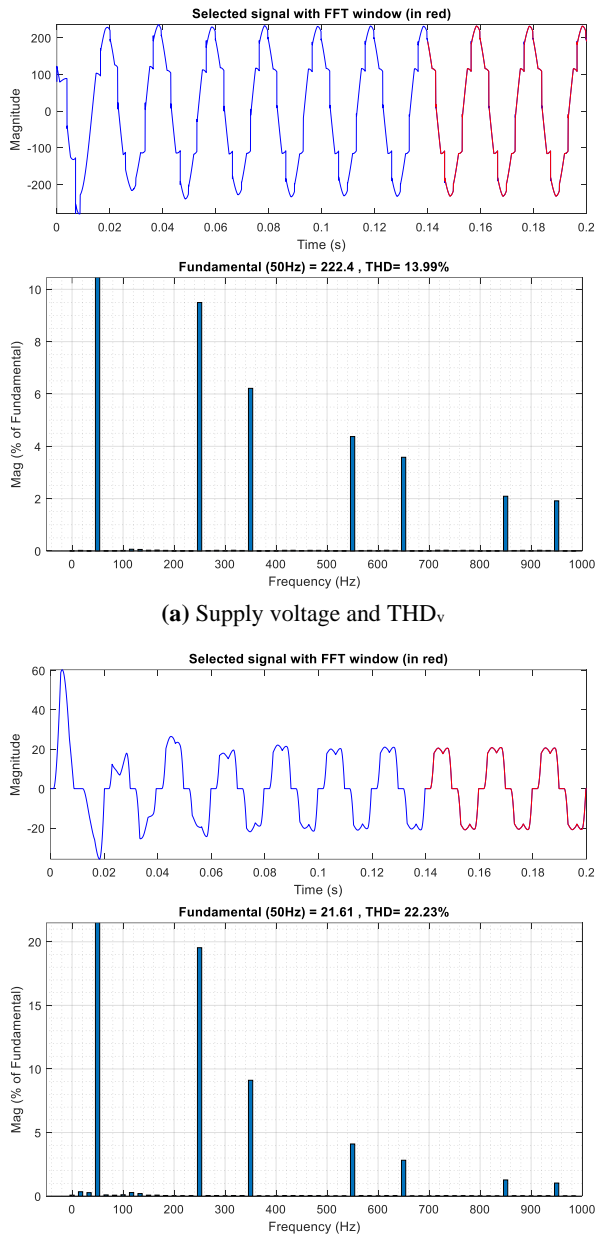


Figure 6. THD values without C-type filter

Figure 8 indicates that performance of the battery charging process enhances as compared to without filter operation. As mentioned in [35], after compensation and harmonic elimination, the dc voltage may be higher for an uncontrolled rectifier. A slight increase in V_{dc} yields a large increase in the output power. It is clearly seen from the Figure 9 that with the mitigation of harmonics and power factor improvement, output voltage of converter structure increases from 388.4 to 388.58 V_{dc} on average. This observation is reflected in battery charging current too, while the input power is maintained constant, charging current increases from 18 A to 23 A on average. The small change in charging voltage (0.18 V_{dc}) leads an increase of 5 A which can be calculated by change in V_{dc} / battery internal resistance (0.18 V_{dc} /0.036 Ω). It can be concluded that speed of the battery charging

process under the same operation conditions increases by 21% in case of using C-type filter. Therefore, the SoC curve as shown in Figure 8a goes up faster than without filter operation during the charging (Figure 5a).

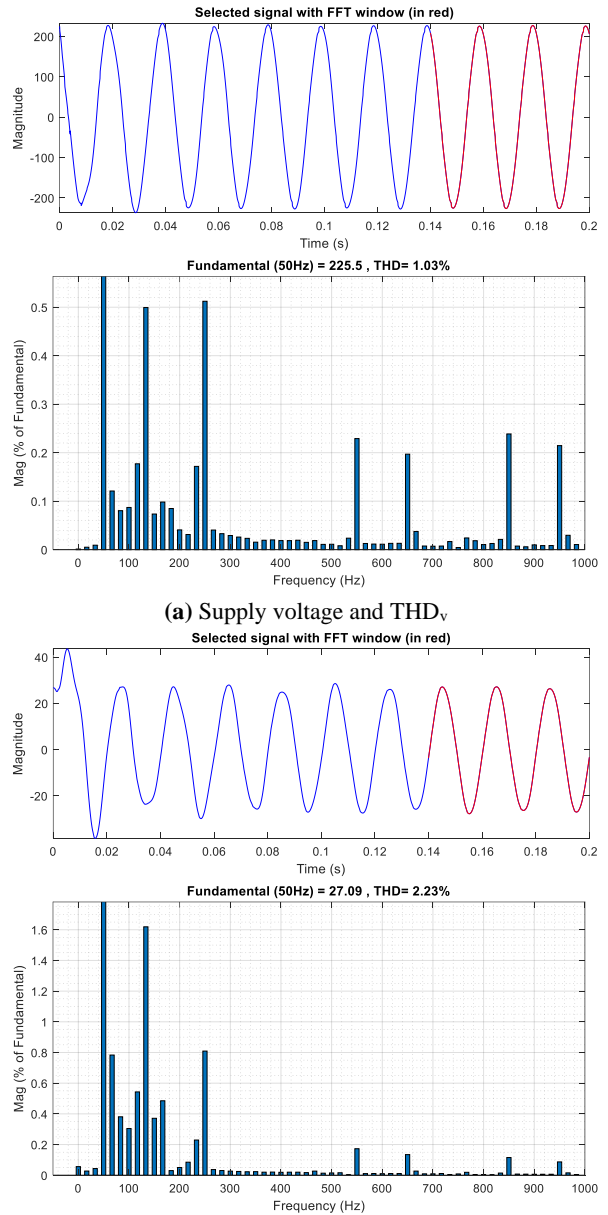


Figure 7. THD values with C-type filter

7. Conclusion

WPT systems are widely employed in EVCS. However, structure of WPT causes current with harmonics and thus causes non-sinusoidal voltage drops. In this study, SVM-based optimal C-type passive filter design problem is taken into account in order to mitigate these harmonics and to increase PF. Therefore, firstly modeling of EVCS is realized by utilizing filter coefficients as inputs where THD_i, THD_v, PF are chosen as outputs. Secondly, PSO algorithm is employed on the SVM to find best filter parameters.

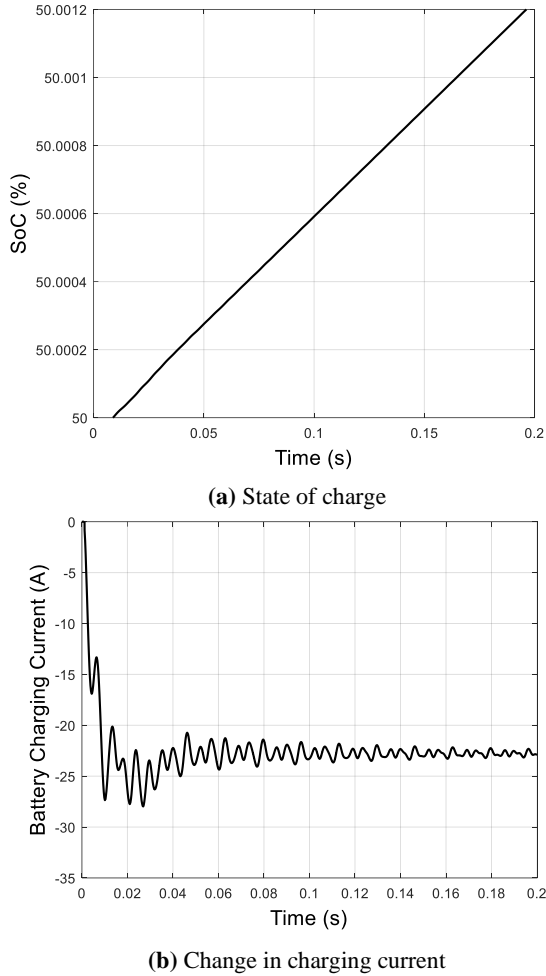


Figure 8. Charging of the battery with C-type filter

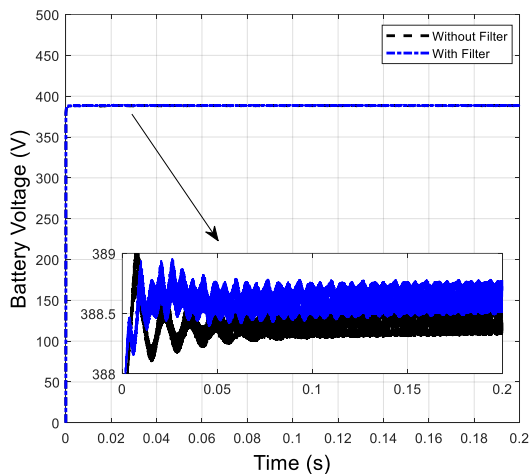


Figure 9. Comparison of charging voltage values with and without filter operation

The main advantage of the presented method is that it does not require any equivalent circuit parameters of the WPT system while determining the filter parameters. However, a single-output FF is employed in this study which is the main drawback of the method. It does not have the capability to find solutions in all objective contributions. After successful modelling and

optimization process, the designed filter is employed in EVCS by using Matlab®/Simulink™ environment. Simulation results prove that THD_v and THD_i decrease under the limits defined by IEEE Standard 519-2014 and PF approaches to 1. Future works will be directed to compare different types of passive filter structures as well as various optimization methods such as chaotic PSO for the purpose of mitigating harmonics in WPT system.

Acknowledgments

The author would like to thank the anonymous reviewers for their valuable comments. This work was funded by Balikesir University under research grant BAP 2022/079.

References

- [1] Demirtas, M., Calgan, H., & Ilten, E. (2022). Elektrikli Araçlar için Şebekeden bağımsız Kablosuz Şarj İstasyonu Tasarımı, *Mühendislikte Araştırma ve Değerlendirmeler*. Gece Kitaplığı, 241–266.
- [2] Yağcıtekin, B., Uzunoğlu, M. & Karakaş, A. (2011). Elektrikli araçların şarjı ve dağıtım sistemi üzerine etkileri. *Elektronik ve Bilgisayar Sempozyumu, Fırat Üniversitesi-Elazığ*, 316-320.
- [3] Güneş, D., Tekdemir, İ. G., Karaarslan, M. Ş., & Alboyacı, B. (2018). Assessment of the impact of electric vehicle charge station loads on reliability indices. *Journal of the Faculty of Engineering and Architecture of Gazi University*, 33(3), 1073-1084.
- [4] Alonso, M., Amaris, H., Germain, J. G., & Galan, J. M. (2014). Optimal charging scheduling of electric vehicles in smart grids by heuristic algorithms. *Energies*, 7(4), 2449-2475.
- [5] Spaur, C. W. , Braitberg, M. F., Kennedy, P. J., & Hatcher, L. B. (1998). Mobile portable wireless communication system. Google Patents.
- [6] Li, S., & Mi, C. C. (2014). Wireless power transfer for electric vehicle applications. *IEEE Journal of Emerging and Selected Topics in Power Electronics*, 3(1), 4-17.
- [7] Musavi, F., & Eberle, W. (2014). Overview of wireless power transfer technologies for electric vehicle battery charging. *IET Power Electronics*, 7(1), 60-66.
- [8] Sun, L., Ma, D., & Tang, H. (2018). A review of recent trends in wireless power transfer technology and its applications in electric vehicle wireless charging. *Renewable and Sustainable Energy Reviews*, 91, 490-503.
- [9] Liu, J., Xu, F., Sun, C., & Loo, K. H. (2022). A Compact Single-Phase AC–DC Wireless Power Transfer Converter With Active Power Factor Correction. *IEEE Transactions on Industrial Electronics*, 70(4), 3685-3696.
- [10] Gündüz, H., Demirtas, M., Ilten, E., & Calgan, H. (2020). Paralel aktif güç filtresi için bulanık

- uyarlamalı kesirli PI denetleyici tasarımı. *Düzce Üniversitesi Bilim ve Teknoloji Dergisi*, 8(3), 1975-1994.
- [11] Yang, W., Wang, J., Zhang, Z., & Gao, Y. (2012). Simulation of electric vehicle charging station and harmonic treatment. In *2012 International Conference on Systems and Informatics* (pp. 609-613).
- [12] Zhao, G., & Yue, Y. (2017). Harmonic analysis and suppression of electric vehicle charging station. *IEEE International Conference on Mechatronics and Automation* (pp. 347-351).
- [13] Khudher, S. M., Aris, I. B., Othman, M., & Mailah, N. (2021). Output-Input Hybrid Passive Filter Design for Electric Vehicle Charging Station. *Al-Rafidain Engineering Journal (AREJ)*, 26(2), 132-142.
- [14] Balci, M. E. (2014). Optimal C-type filter design to maximize transformer's loading capability under non-sinusoidal conditions. *Electric Power Components and Systems*, 42(14), 1565-1575.
- [15] Karadeniz, A., & Balci, M. E. (2018). Comparative evaluation of common passive filter types regarding maximization of transformer's loading capability under non-sinusoidal conditions. *Electric Power Systems Research*, 158, 324-334.
- [16] Lange, A. G., & Redlarski, G. (2020). Selection of C-type filters for reactive power compensation and filtration of higher harmonics injected into the transmission system by arc furnaces. *Energies*, 13(9), 2330.
- [17] Habibolahzadeh, M., Mahdinia Roudsari, H., Jalilian, A., & Jamali, S. (2021). Using C-type filter with partial compensation method for capacity reduction of hybrid power quality conditioner in co-phase traction power system. *IET Power Electronics*, 14(14), 2350-2373.
- [18] Balci, M. E., & Karaoglan, A. D. (2013). Optimal design of C-type passive filters based on response surface methodology for typical industrial power systems. *Electric Power Components and Systems*, 41(7), 653-668.
- [19] Ozdemir, S., Demirtas, M., & Aydin, S. (2016). Harmonic Estimation Based Support Vector Machine For Typical Power Systems. *Neural Network World*, 26(3), 233-252.
- [20] Koizumi, H., & Kurokawa, K. (2007). Analysis of the class DE inverter with thinned-out driving patterns. *IEEE Transactions on Industrial Electronics*, 54(2), 1150-1160.
- [21] Hu, J., & Zhao, J. (2020). Design of wireless power transfer system with inputfilter. *IET Power Electronics*, 13(7), 1393-1402.
- [22] Sis, S. A., & Akca, H. (2020). Maximizing the efficiency of wireless power transfer systems with an optimal duty cycle operation. *AEU-International Journal of Electronics and Communications*, 116, 153081.
- [23] Calgan, H., Ilten, E., & Demirtas, M. (2020). Thyristor controlled reactor-based voltage and frequency regulation of a three-phase self-excited induction generator feeding unbalanced load. *International Transactions on Electrical Energy Systems*, 30(6), e12387.
- [24] Xiao, Y., Zhao, J., & Mao, S. (2004). Theory for the design of C-type filter. *11th International Conference on Harmonics and Quality of Power*, (pp. 11-15).
- [25] Ilten, E., & Demirtas, M. (2016). Off-Line Tuning of Fractional Order PI λ Controller by Using Response Surface Method for Induction Motor Speed Control. *Journal of Control Engineering and Applied Informatics*, 18(2), 20-27.
- [26] Demirtas, M., Ilten, E., & Calgan, H. (2019). Pareto-based multi-objective optimization for fractional order PI λ speed control of induction motor by using Elman neural network. *Arabian Journal for Science and Engineering*, 44(3), 2165-2175.
- [27] Ilten, E., Calgan, H., & Demirtas, M. (2022). Design of induction motor speed observer based on long short-term memory. *Neural Computing and Applications*, 34(21), 18703-18723.
- [28] Cortes, C., & Vapnik, V. (1995). Support-vector networks. *Machine Learning*, 20, 273-297.
- [29] Pala, M. A., Çimen, M. E., Akgül, A., Yıldız, M. Z., & Boz, A. F. (2022). Fractal dimension-based viability analysis of cancer cell lines in lens-free holographic microscopy via machine learning. *The European Physical Journal Special Topics*, 231(5), 1023-1034.
- [30] Türkan, Y. S., Aydoğmuş, H. Y., & Erdal, H. (2016). The prediction of the wind speed at different heights by machine learning methods. *An International Journal of Optimization and Control: Theories & Applications (IJOCTA)*, 6(2), 179-187.
- [31] Taibi, D., Amieur, T., Laamayad, T., & Sedraoui, M. (2022). Improvement of the Standard Perturb & Observe MPPT control strategy by the proposed Fuzzy Logic Mechanism for a Cascade Regulation of a PMSM-based PV pumping system. *Arabian Journal for Science and Engineering*, 1-17.
- [32] Ilten, E. (2022). Conformable fractional order controller design and optimization for sensorless control of induction motor. *COMPEL: Int Journal for Computation and Mathematics in Electrical and Electronic Engineering*, 41(5), 1528-1541.
- [33] Kilic, F., Sezen, S., & Sis, S. A. (2020). A misalignment-adaptive wireless power transfer system using PSO-based frequency tracking. *An International Journal of Optimization and Control: Theories & Applications (IJOCTA)*, 10(2), 206-217.
- [34] I. F. II (2014). IEEE Recommended Practice and Requirements for Harmonic Control in Electric Power Systems, in *IEEE Std 519-2014* (Revision of

IEEE Std 519-1992).

- [35] Balcı, M. E., & Emanuel, A. E. (2011). Apparent power definitions: a comparison study. *International Review of Electrical Engineering*, 6, 2713–2722.

Haris Calgan received Ph.D. Degree in Electrical-Electronics Engineering from Balıkesir University (Turkey) in 2020. His research interests are robust control, artificial intelligence, renewable energy. From 2014 till now, he is working as research assistant at Balıkesir University (Turkey).

 <http://orcid.org/0000-0002-9106-8144>

An International Journal of Optimization and Control: Theories & Applications (<http://ijocta.balikesir.edu.tr>)



This work is licensed under a Creative Commons Attribution 4.0 International License. The authors retain ownership of the copyright for their article, but they allow anyone to download, reuse, reprint, modify, distribute, and/or copy articles in IJOCTA, so long as the original authors and source are credited. To see the complete license contents, please visit <http://creativecommons.org/licenses/by/4.0/>.